Title
Preliminary Studies of the Impact of CXCL12 on the Foreign Body Reaction to Pancreatic Islets Microencapsulated in Alginate in Nonhuman Primates

Journal
Transplantation Direct, 5(5)

ISSN
2373-8731

Authors
Sremac, Marinko
Lei, Ji
Penson, Madeline FE
et al.

Publication Date
2019-05-01

DOI
10.1097/txd.0000000000000890

OPEN

Preliminary Studies of the Impact of CXCL12 on the Foreign Body Reaction to Pancreatic Islets Microencapsulated in Alginate in Nonhuman Primates

Marinko Sremac, PhD,[1] Ji Lei, MD,[2] Madeline F.E. Penson, BS,[1] Christian Schuetz, MD,[2] Jonathan R.T. Lakey, PhD,[3] Klearchos K. Papas, PhD,[4] Pushkar S. Varde, PhD,[5] Bernhard Hering, MD[6] Paul de Vos, PhD,[7] Timothy Brauns, MBA,[1] James Markmann, MD, PhD,[2] and Mark C. Poznansky, MD, PhD,[1]

Background. We previously demonstrated that the incorporation of the chemokine CXCL12 into alginate microbeads supported long-term survival of microencapsulated auto-, allo-, and xenogeneic islets in murine models of diabetes without systemic immune suppression. The purpose of this study was to test whether CXCL12 could abrogate foreign body responses (FBRs) against alginate microbeads which were empty or contained autologous islets in healthy nonhuman primates (NHPs; n = 4). **Methods.** Two NHPs received intraperitoneal implants of 400 000 alginate microbeads with or without CXCL12, and postimplantation immunological and histopathological changes were evaluated up to 6 months postimplantation. A similar evaluation of autologous islets in CXCL12-containing alginate microbeads was performed in NHPs (n = 2). **Results.** CXCL12-containing alginate microbeads were associated with a markedly reduced FBR to microbeads. Host responses to microbead implants were minimal, as assessed by clinical observations, blood counts, and chemistry. Evaluation of encapsulated islets was limited by the development of necrotizing pancreatitis after hemipancreatectomy in 1 NHP. A limited number of functioning islets were detectable at 6 months posttransplantation in the second NHP. In general, empty microbeads or islet-containing beads were found to be evenly distributed through the intraperitoneal cavity and did not accumulate in the Pouch of Douglas. **Conclusions.** Inclusion of CXCL12 in alginate microbeads minimized localized FBR. The NHP autologous islet implant model had limited utility for excluding inflammatory/immune responses to implanted islets because of the complexity of pancreatic surgery (hemipancreatectomy) before transplantation and the need to microencapsulate and transplant encapsulated autologous islets immediately after pancreatectomy and islet isolation.

(*Transplantation Direct* 2019;5:e447; doi: 10.1097/TXD.0000000000000890. Published online 15 April, 2019.)

Received 8 February 2019. Accepted 4 March 2019.

[1] Department of Infectious Diseases, Vaccine and Immunotherapy Center, Massachusetts General Hospital, Boston, MA.

[2] Division of Transplant Surgery, The Pancreas/Islet Transplant Program, Massachusetts General Hospital, Boston, MA.

[3] Clinical Islet Program, Surgery School of Medicine, University of California Irvine, Irvine, CA.

[4] Department of Surgery, Institute for Cellular Transplantation, University of Arizona, Tucson, AZ.

[5] ViCapsys, Inc., Athens, GA.

[6] Department of Surgery, University of Minnesota, Minneapolis, MN.

[7] Department of Pathology and Medical Biology, University of Groningen, Groningen, The Netherlands.

M.S. performed the experiments, analyzed the data, participated in writing and editing of the manuscript, and provided substantial contributions to the conception and design of the work, acquisition, analysis, and interpretation of data. J.L. performed pre- and postsurgery clinical care of NHPs, donor pancreas recovery surgery, and isolated NHP islets, performed transplantation of microbeads, and designed the NHP research protocol and surgical procedure. M.F.E.P. performed experiments and analyzed the data. C.S. performed pretransplant and posttransplant care of the animals. J.R.T.L. provided the consultation on study design and encapsulation protocols. K.K.P. provided the consultation in designing the study. P.S.V. provided the consultation in the analysis of microbeads. P.d.V. and B.H. provided the consultation in designing the study. T.B. participated in project management, designed the study, and edited the article, contributed to the design of experiments, interpretation of results, and writing of the manuscript. J.M. performed the transplantation of microbeads and contributed to the design of the study. M.C.P. directed the study and provided substantial contributions to the conception and design of the work, participated in drafting the work and revised it critically for important intellectual content, participated in the writing and editing of the manuscript, and was responsible for the final approval of the version to be published.

M.S. and J.L. contributed equally to this manuscript.

M.C.P. is the scientific founder of ViCapsys. J.M. was a scientific consultant to ViCapsys.

The present work was supported by the JDRF (grant 2-SRA-2014-290-Q-R) and the VIC Innovation Fund.

Supplemental digital content (SDC) is available for this article. Direct URL citations appear in the printed text, and links to the digital files are provided in the HTML text of this article on the journal's Web site (www.transplantationdirect.com).

Correspondence: Dr Mark C. Poznansky, MD, PhD, Director, Vaccine and Immunotherapy Center, Massachusetts General Hospital, 149 13th St, Charlestown, MA 02129. (mpoznansky@partners.org).

ISSN: 2373-8731

DOI: 10.1097/TXD.0000000000000890

While insulin replacement therapy has made a significant contribution toward prolonging and enhancing the life of the people with type 1 diabetes, it is not yet an optimal treatment, as it cannot dynamically regulate blood sugar levels with the precision of islets. Over the last 30 years, allogeneic islet transplantation has become a firmly established treatment modality that may soon receive regulatory approval for clinical use.[1] Nevertheless, its potential impact is limited by the scarcity of suitable deceased-donor islets and the need to provide recipients lifelong systemic immune suppression therapy to prevent islet rejection.

These limitations have led investigators to explore the use of alternative islet replacement sources like porcine islets, which do not have supply limitations, and to replace systemic immune suppression with localized immune protection. One embodiment of this approach is enclosure of the islet within microspheres of a biocompatible polymer or polymers. Alginate, a natural polymer derived from brown seaweed, has emerged as a leading candidate for this approach, as it can be readily formed into such microspheres, its biocompatibility has been tested in a range of animal models,[2-6] and it has been used for implantation or injection in several approved or clinical stage therapeutics.[7-10] Numerous studies have guided investigators toward utilization of high-purity forms of alginate as a means of minimizing unwanted foreign body reactions and immune responses[11-15] and to capsule designs incorporating polylysine or polyornithine shells that can exclude the passage of larger unwanted immune proteins.[16,17]

We have previously explored the incorporation of a recombinant form of the human chemokine CXCL12 alpha (CXCL12) into alginate microbeads as a means of providing a long-term, site-specific, immunoprotective, and prosurvival environment for both allogeneic and xenogeneic islets. At local concentrations of 1 μg/mL, CXCL12 has been shown to selectively repel effector T cells while continuing to recruit and retain immune-suppressive regulatory T cells to an anatomic site in models of transplantation and cancer.[18,19] In an immunocompetent diabetic mouse model, implantation of simple alginate microbeads containing allogeneic and xenogeneic islets and CXCL12 with a starting concentration of 1 μg/mL extended euglycemia to >300 days compared with microbeads without or with lower concentrations of CXCL12.[5]

In addition to its immunomodulatory effects, CXCL12 has also been shown to play a role in reducing inflammatory responses at sites of injury,[20,21] to promote healing through the recruitment of endothelial progenitor cells,[22-24] and to act as a prosurvival signal for beta cells.[25] CXCL12 is also likely to attract stem cells that further modify the environment around the microbead toward healing[26,27] and immune tolerance.[28] Thus, CXCL12 has "multimodal" potential to extended survival and function for implanted islets. In this context, we use simple microbeads of ultrapure alginate, which not only provide a supportive and protective matrix for islets but also enable prolonged release of CXCL12 to enhance islet survival while dampening inflammatory responses and promoting immune tolerance of the islet-containing microbeads. In this study, we set out to examine in a stepwise manner whether data in mice could be reproduced in nonhuman primates (NHPs)—commencing with a study of intraperitoneal (IP) implantation of alginate microbeads with and without CXCL12 and subsequently alginate microbeads containing autologous islets with CXCL12.

Results from these preliminary studies suggest that in NHPs, implants of CXCL12-containing microbeads were well tolerated and that the chemokine modulates host innate immune responses toward the alginate microbeads. However, we found that the use of an autologous islet implant model to isolate immune effects against the alginate microbead was undermined by the immune activating effects of the surgery itself, the inability to culture autologous islets over prolonged periods of time to reduce antigenicity from dying islets, and the development of significant postsurgical pancreatitis in 1 animal. Overall, these studies provide the support for continued testing of the use of CXCL12 in alginate microbeads to encapsulate allogeneic and xenogeneic islets and to identify key parameters that can maximize the success of follow-on transplantation studies. In addition, our study highlights the complexities and potential confounding factors generated in the autologous islet transplant model in NHPs.

MATERIALS AND METHODS

Ultrapurified Alginate and Its Characterization

We utilized ultrapure low-viscosity, high-mannuronic acid (LVM) alginate produced under current Good Manufacturing Practice conditions (FMC Biopolymers/NovaMatrix, Lot #BP-1410–28). A number of key characteristics of the alginate reported in the certificate of analysis, including purity, endotoxin levels, mannuronic acid concentration, and apparent and dynamic viscosity, were verified by our laboratory or by other investigators. We evaluated the level of endotoxins in both unfiltered and sterile-filtered (0.8/0.2-μm filter) alginate using the Endosafe PTS (Charles River Laboratories) detection system in accordance with a standard operating procedure derived from the manufacturer's instructions. Further analyses of the immunoactivating potential of the alginate were performed using established in vitro HEK-Blue and THP-1 cell activation assays and quantitative ELISAs to identify the concentrations of lipopolysaccharides, peptidoglycan, lipoteichoic acid, and flagellin within the alginate. These assays were performed in accordance with published procedures.[29]

Characterization of Recombinant Human CXCL12

We used recombinant human CXCL12 reconstituted in sterile normal saline at a concentration of 1 μg/mL throughout this study (Peprotech, Lot #300-28A). The purity and identity of the protein was confirmed by 21st Century Biochemicals (Marlborough, MA) utilizing high-performance liquid chromatography and liquid chromatography–mass spectrometry. Endotoxin contamination of this bacterially expressed chemokine was evaluated using the Endosafe PTS assay.

Production of Alginate Encapsulation Solution

Ultrapure low-viscosity, high-mannuronic acid alginate was used to produce microbeads with and without CXCL12 and with CXCL12 and autologous primate islets. A 1.6%-weight per volume sodium alginate solution was prepared by mixing the alginate with an endotoxin-free 300-mOsmol sodium chloride (NaCl) solution (Sigma, Cat #5150-1L) and passed through a 0.8/0.2-μm sterile syringe filter (Pall Life Sciences, Cat #4658). For preparations that incorporated CXCL12, the chemokine was dissolved in 300 mOsmol NaCl and mixed with alginate to produce a resultant solution with a chemokine concentration of 1 μg/mL weight to volume of alginate solution.

NHP Pancreatic Islet Isolation

Donor islets were isolated from pancreatic tissue following a hemipancreatectomy procedure on the donor/recipient NHP. The protocol of islet isolation was based on a modified human islet isolation method (**Materials and Methods S1, SDC,** http://links.lww.com/TXD/A205).

Production and Characterization of Alginate Microbeads

The B-395 Pro Encapsulator (Buchi Corporation, New Castle, DE) was used to produce all microbeads for this study. We produced the empty microbeads and the first autologous islet-containing microbeads using a vibrational encapsulation technique with a 200- or 300-µm nozzle.[30,31] For the second set of autologous islet microbeads, an airflow technique with a 400-µm air-dripping nozzle was used (**Materials and Methods S2, SDC,** http://links.lww.com/TXD/A205).

NHPs and Surgical Procedure for Microbead Implantation and Partial Pancreatectomy

NHPs (male 1- to 2-year-old Mauritian origin cynomolgus monkeys) were obtained from Charles River Laboratories (Houston, TX). IP implantation of empty microbeads was performed using a minimally invasive technique with healthy male cynomolgus monkeys (*Macaca fascicularis*), 2 to 3 years old, 4–5 kg. One NHP received microbeads without CXCL12 (–), and a second NHP received microbeads with CXCL12 (+). Surgeons and pathologists were blinded to the CXCL12 content of the implant. All procedures and the protocol followed were approved by the Center for Comparative Medicine at Massachusetts General Hospital. Surgical evaluation of NHPs peritoneum and explant of free and embedded microbeads were done at 1, 3, and 6 months after microbead implantation (**Materials and Methods S3, SDC,** http://links.lww.com/TXD/A205).

NHP Plasma, Serum Collection, and PBMC Isolation

Blood samples were taken from the NHPs before surgery (days –7 and 0) and posttransplantation in weeks 1–4, 13, and 26. Plasma and intra-abdominal aspirate samples were analyzed for the levels of 14 different cytokines and CXCL12. Peripheral blood mononuclear cells (PBMCs) from the blood samples were analyzed by flow cytometry (**Materials and Methods S4, SDC,** http://links.lww.com/TXD/A205).

Islet Functional Studies

Static glucose stimulation index assays were performed on fresh-isolated, fresh-encapsulated, and aspirated encapsulated islets using low- (1.67 mM) and high-glucose (16.7 mM) solutions. Approximately the same number (10–20) of islets were incubated for 60 and 90 minutes in low and high glucose, respectively, and the supernatants were collected and stored for subsequent C-peptide analysis via ELISA following the manufacturer's protocol.

RESULTS

Preimplantation Characteristics of Components and Microbeads

Alginate Immunogenicity

Immunogenic potential of the alginate included the assessment of endotoxin levels with the EndoSafe assay and ELISA-based quantitation of other immunocontaminants and a cell-based assay to gauge pathogen-associated molecular pattern–based immunostimulatory potential. Testing in a THP1-XBlue-MD2-CD14 cell line showed that the alginate increased activation of NF-κB/AP-1 when compared with the control sample (Figure S1A, **SDC,** http://links.lww.com/TXD/A205). Additional testing of the biological activity of the peptidoglycan with HEK-Blue cell lines overexpressing Toll-like receptor-2 (TLR-2) showed that the alginate had TLR2-stimulating effects (Figure S1B, **SDC,** http://links.lww.com/TXD/A205). Finally, the quantitative ELISA for lipopolysaccharide in the starting alginate material was under the limit of detection (4.1 ng/mL), and the levels for the alginate postfiltration were below 1 EU/mL. Levels of lipoteichoic acid and flagellin were not detectable (Figure S1C, **SDC,** http://links.lww.com/TXD/A205). However, the peptidoglycan level was 0.4 ng/mL and evaluated as being higher than the desirable limit of <0.1 ng/mL. Overall, the alginate to be used in the study had a relatively low immunogenicity profile but contained immunocontaminants with the potential to stimulate innate immune responses.

CXCL12 Purity and Potency

Two different sources of recombinant human CXCL12 were analyzed for potential use in this study: CXCL12 produced by Peprotech, Inc. (Rocky Hill, New Jersey) using an *E coli* expression system and CXCL12 from Almac (Craigavon, United Kingdom), which is produced using solid-state peptide synthesis techniques (**Results S5, SDC,** http://links.lww.com/TXD/A205).

Empty Microbead Morphology

Two batches of approximately 400 000 empty alginate microbeads each were produced, 1 with and 1 without CXCL12. The size and roundness of these microbeads were assessed. The resulting size and shape of the microbeads did not appear to be affected by the presence of CXCL12. Microbeads without CXCL12 (sample A) had a mean diameter of 426.55 ± 27.36 µm with a circularity of 0.78 ± 0.13, while microbeads with CXCL12 (sample B) had a mean diameter of 428.27 ± 37.23 µm with a circularity of 0.80 ± 0.12 (Figure 1A and B).

Preimplantation porosity studies on these microbeads using a dextran diffusion analysis after 30 minutes demonstrated an increase in fluorescence intensity for all 3 preconjugated dextrans. Penetration rates were 90% CXCL12 (–) and 95% CXCL12 (+) for the 10 kDa dextran, 55% for both samples with 150 kDa dextran, and 30% for both samples with the 500 kDa dextran (Figure S2A, **SDC,** http://links.lww.com/TXD/A205). At the 1-month assessment, 30-minute microbead permeability declined significantly for the 10 kDa dextran (~70%), while the 150 kDa dextrans declined ~20% and the 500 kDa declined ~40% (Figure S2B, **SDC,** http://links.lww.com/TXD/A205).

Autologous Islet Microbead Production, Size, and Shape

For the production of autologous islet microbeads, to minimize the number of nonislet-containing microbeads, the volume of alginate solution applied was based on the volume of provided islets. About 40 000 islet equivalents were isolated from the hemipancreatectomy on the first

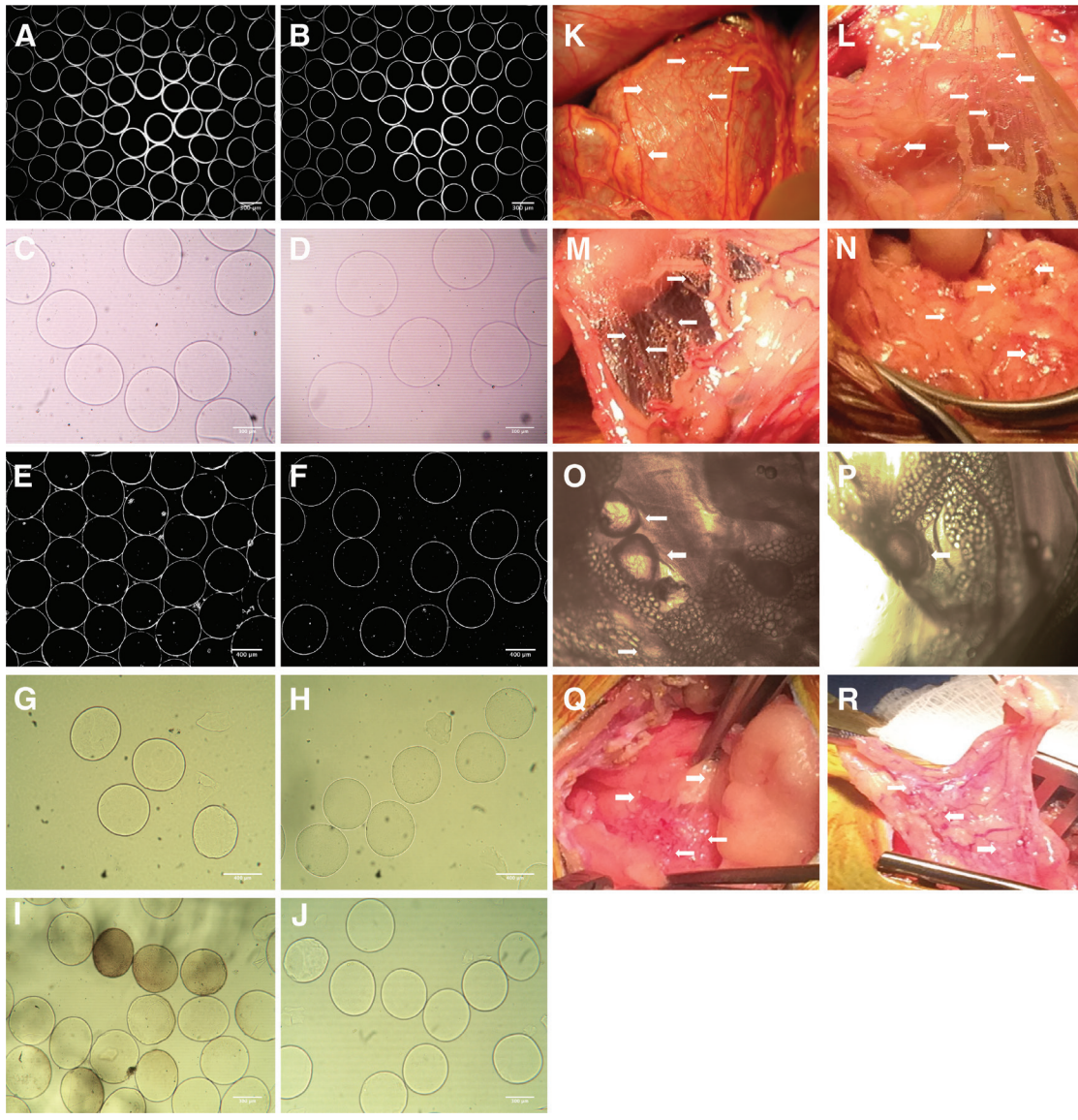

FIGURE 1. Images of the original empty microbeads preimplantation and appearance of retrieved microbeads postexplant, together with the gross surgical appearance at the specific time points. Set of the preimplantation microbeads used for the NHP implants are shown (A) without CXCL12 (–) and (B) with CXCL12 (+). Size and shape of the microbeads were very similar between the CXCL12 (–) and CXCL12 (+) samples, magnification ×4. Images of the microbeads postexplant at day 30 are shown (C) without CXCL12 (–) and (D) with CXCL12 (+). Similar images shown in A–B and E–F were used by University of California Irvine and their software program for the microbeads size and shape evaluation. Explanted microbeads at day 90 are shown (G) without CXCL12 (–) and (H) with CXCL12 (+). Microbeads measured 500–530 μm in diameter, magnification ×10. Explanted microbeads at day 180 are shown (I) without CXCL12 (–) and (J) with CXCL12 (+). Microbeads explanted from the CXCL12 (–) NHP were in the range of 480 ± 43 μm, and some microbeads appear to have a pigmentation with changed surface but without obvious cell infiltration. Microbeads from the CXCL12 (+) NHP were in the range of 485 ± 12 μm, magnification ×10. Images from the surgical appearance of microbeads (shown with arrows) at days 30, 90, and 180 demonstrate visible numerous concentrations of microbeads within the peritoneal cavity of NHPs (K) without CXCL12 (–) and (L) with CXCL12 (+) at day 30. M, Image of the omental tissue with CXCL12 (–) NHP demonstrates the cluster of microbeads (N) with CXCL12 (+) NHP at day 90. Microscopic images of the tissues with embedded empty microbeads from the CXCL12 (–) explant at day 180 are shown with arrows in O–P, demonstrating the "vesicle-like" pouch around the single microbeads with a visible vascularization, and tissues with embedded empty microbeads from the CXCL12 (+) are seen in Q and R. NHP, nonhuman primate.

NHP (**Results S6;** Figure S3A–C, **SDC,** http://links.lww.com/TXD/A205). For the production of autologous islet microbeads from the second NHP hemipancreatectomy, we utilized an airflow encapsulation process with a 400-μm air-dripping nozzle, and the encapsulator settings were optimized for this process (**Results S6;** Figure S3G–S3I, **SDC,** http://links.lww.com/TXD/A205).

Postimplantation Effects of Empty Microbead Implants

Overall Animal Health During Study

Both NHPs receiving the empty microbead implants recovered quickly from surgery and appeared healthy during the entire period of the study. Neither NHP had any significant changes in behavior, appetite, or weight, nor were there any abnormal complete blood count with differential or serum chemistry results over the 6 months of the study (data not shown).

Changes to Free Microbeads

At the 1-month assessment, we instilled a single 100-mL normal saline lavage in each NHP and aspirated a roughly equal amount of microbeads from each animal, representing 53%–56% of the original implant volume. During the procedure, a sample of these aspirated microbeads was examined using phase contrast microscopy. These microbeads appeared to have a normal morphology and appearance without significant aggregation and were clearly transilluminable without evident cellular infiltrate on the surface of the microbeads. A second sample of the microbeads from each NHP were imaged and measured several hours after the removal (Figure 1C and D). These showed an increase in median diameter compared with the size measured before implantation. CXLC12 (–) microbeads had increased in size by 33.8% (median = 570 μm), while CXCL12 (+) had increased by 44.3% (median = 609 μm). Images of these microbeads were also sent to University of California Irvine for assessment (Figure 1E and F). As these samples had been stored in the lavage solution for several hours before these measurements were taken, it is possible that the beads swelled in the normal saline solution. We subsequently washed and stored a sample of the aspirated microbeads in a 0.9% w/v NaCl solution and imaged them again after an additional 4 weeks. At that time, the CXCL12 (+) microbeads had a mean diameter of 591 μm (38.2% increase in diameter over the implant size), showing that these microbeads had stabilized in a normal saline solution (data not shown).

At the 3-month evaluation, free microbeads were seen throughout the peritoneal cavity of both animals, and there were again no visible indications of embedded beads in either animal and in particular in the Pouch of Douglas. A single 30-mL lavage released a small volume of microbeads from either animal (~300 μL of microbeads from the CXCL12 [–] implant and ~230 μL of microbeads from the CXCL12 [+] implant), amounting to only 2000–5000 microbeads in each case. Measurements were done on 50 microbeads using the captured images and the ImageJ software. Microbeads without CXCL12 (–) had a mean diameter of 499.67 ± 17.98 μm with a circularity of 0.9598, while microbeads with CXCL12 (+) had a mean diameter of 509.16±14.56 μm with a circularity of 0.9698. There was no significant difference in the size between these 2 samples of microbeads. Also, the number of recovered microbeads from lavage was small; therefore, we did not provide a graph representing these measurements. Because many microbeads were visible in the peritoneum, it is not clear why the number of microbeads recovered from the lavage was small. This could have been due to the use of a smaller volume of IP lavage (30 mL) and the minimal effort taken to remove beads from the peritoneum to minimize the disruption of the tissues, or due to more significant adherence of the beads on the surface of the peritoneal tissue. Microbeads recovered from the CXCL12 (–) implant showed some signs of degradation as indicated by a loss of circularity and change in the shape (Figure 1G), while microbeads from the CXCL12 (+) implant were without damage and remained more circular (Figure 1H).

At the 6-month time point, about 500 μL of free microbeads was recovered from the peritoneal lavage of the CXCL12 (–) animal and ~200 μL from the CXCL12 (+) animal. The CXCL12 (–) microbeads were more variable in size (491.55 ± 45.9 μm) than the CXCL12 (+) microbeads (501.81 ± 22.69 μm); a minority of CXCL12 (–) microbeads showed change in transparency (7.55%), and 1.89% showed cellularization on the surface. In contrast, the CXCL12 (+) microbeads were round, relatively uniform in size, clear, and not cellularized. Samples of each microbead were first imaged (Figure 1I and J) and then placed in a culture media to observe the possible additional changes during an extended period of time. It is very likely that microbeads picked up a pigment in the animals, perhaps related to a foreign body reaction. The CXCL12 (–) samples became discolored even more during the period of 7–10 days, while the CXCL12 (+) microbeads remained transparent and translucent without pigmentation (data not shown). Again, microbeads were found throughout the peritoneal cavity and did not accumulate or aggregate to any detectable extent in the Pouch of Douglas.

Changes to Peritoneum

At the 1-month surgical evaluation, visual inspection did not show any intra-abdominal inflammation or physical evidence of adhesions in either NHP (Figure 1K and L). In both animals, the microbeads appeared distributed throughout the peritoneum and were lightly adherent to tissue surfaces with no sign of concentration in the pelvic floor. No obvious embedding of microbeads within in the IP tissue was observed. At the 3-month assessment, the NHP receiving the CXCL12 (–) implant showed some evidence of peritoneal adhesions and patchy fibrosis, while the NHP receiving the CXCL12 (+) had no evidence of any IP reaction (Figure 1M and N). At the 6-month assessment point, differences in peritoneal appearance between the 2 animals were more accentuated. In the NHP receiving the CXCL12 (–) implant, additional intra-abdominal adhesions and a patchy fibrosis on scattered surfaces of the peritoneum were seen. At this point, embedded microbeads now appeared for the most part to be surrounded by mesothelial cells as seen in Figure 1O and P. In comparison, the peritoneum of the animal receiving CXCL12 (+) implants looked unchanged from before implantation with no indications of any adhesions or fibrosis (Figure 1Q and R).

Changes to Embedded Microbeads

At the 1-month peritoneal inspection, a number of locations in both animals were noted that had what appeared to be embedded microbeads, and biopsies were taken at these locations (**Results S7, SDC,** http://links.lww.com/TXD/A205; Figure 2A–H). At the 3-month evaluation, several biopsies were taken from random locations, as no embedded beads were evident from a visual inspection (Figure 2I–O). At 6 months, a few samples of each microbead were fixed and prepared for hematoxylin and eosin staining (**Results S7, SDC,** http://links.lww.com/TXD/A205; Figure 2L and P). There were no significant signs of cellularization or fibrosis.

Changes in Plasma and Peritoneal Cytokine and Chemokine Levels

In blood samples drawn both before microbead implantation and at postimplant weeks 1, 2, 3, 4, 13, and 26, only 4 cytokines were measurable in the plasma: interleukin-4 (IL-4), IL-17a, IL-23, and tumor necrosis factor-α. The NHP receiving the CXCL12 (–) implant appeared to have a higher basal activation state for cytokine levels than the NHP with the CXCL12 (+) implant. Both NHPs showed a transient spike in circulating IL-23 between the second and third weeks after implantation. No other changes in cytokine levels compared to baseline measurements either in plasma or in IP aspirate

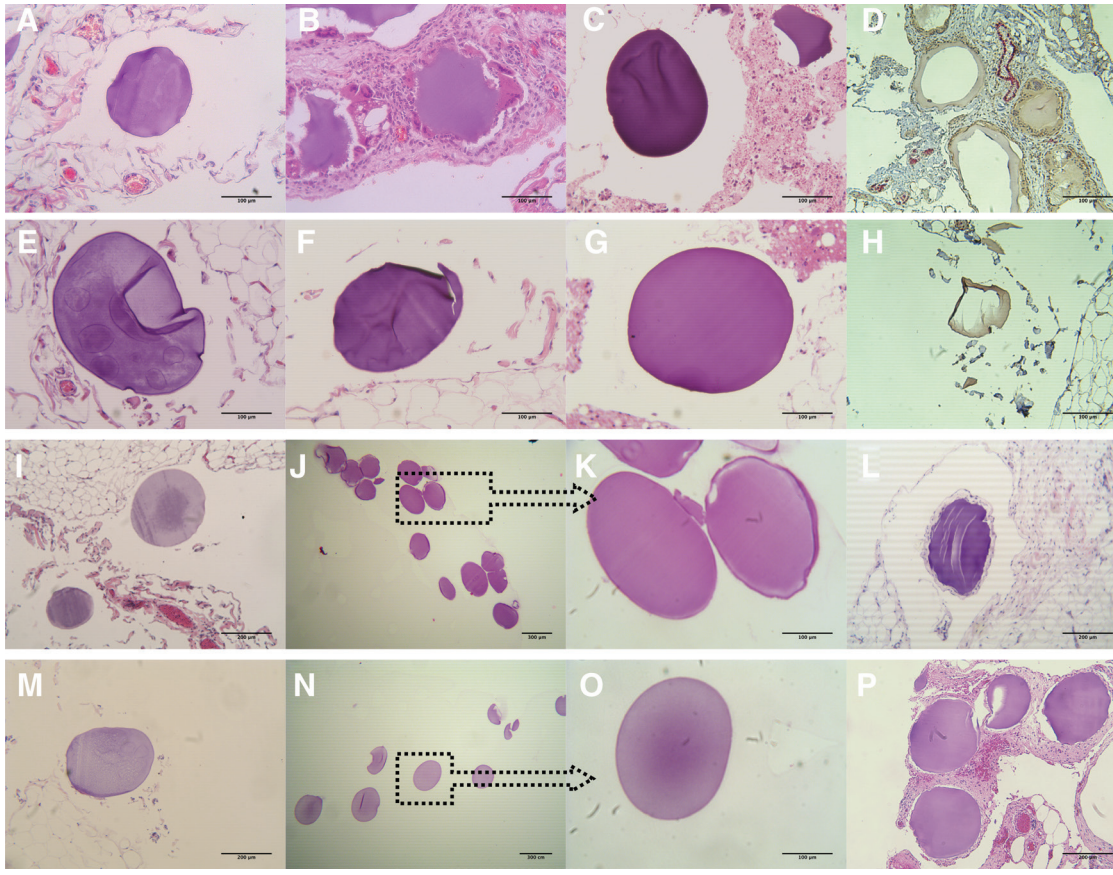

FIGURE 2. Histopathology of the explanted empty microbeads without CXCL12 (–) and with CXCL12 (+) from days 30 to 180. Samples of the microbeads at day 30 are shown in A–H. A, Tissues with embedded microbeads explanted from the NHP without CXCL12 (–). B, Fibrosis of the tissues with microbeads from the CXCL12 (–) NHP. C, Microbead sample found in the aspirate debris. D, IHC staining of the tissues from CXCL12 (–) NHP, stained with antifibroblast activation protein alpha (brown color) and with antimacrophage (red color), magnification ×10. E–G, Tissues with embedded microbeads explanted from the NHP with CXCL12 (+). H, IHC staining of the tissues from CXCL12 (+) NHP, with same staining as for the CXCL12 (–) NHP, magnification ×10. Images showing the explanted tissues (I) and free microbeads (J and K) from CXCL12 (–) NHP and explanted tissues (M) and free microbeads (N and O) from CXCL12 (+) NHP, respectively, at day 90. As it can be seen in the panels with free microbeads, there were no visible cell attachments or fibrosis present in these samples, magnification ×4 and ×20. H&E staining of the explanted tissues from CXCL12 (–) NHP with embedded microbeads at day 180 is shown in image (L) and from CXCL12 (+) NHP shown in image (P), magnification ×10. H&E, hematoxylin and eosin; IHC, immunohistochemistry; NHP, nonhuman primate.

samples (Figure 3A) were seen. The 3- and 6-month plasma and IP aspirate samples from both NHPs showed minimal cytokine changes for granulocyte-macrophage colony-stimulating factor (GM-CSF), IL-18, IL-5, and IL-6 from baseline preimplantation levels (Figure 3B and C). There is a possibility that alginate microbeads being a foreign biological source material to the innate immune system could trigger this cytokine increase. IL-5 is known also to be coexpressed with GM-CSF, which was also elevated in our study. IL-6 can be secreted by macrophages as a proinflammatory cytokine in response to specific microbial molecules.

Plasma and Lavage CXCL12 Levels Postmicrobead Implantation

To evaluate the possible changes in circulating levels of CXCL12 from the implants, we evaluated preimplant samples from 13 different healthy control cynomolgus macaques. The plasma level of CXCL12 ranged between 340 and 620 pg/mL, with an average value of 480.53 pg/mL. Serum levels of CXCL12 in the 2 NHPs receiving empty microbeads on the day of implantation were 500.01 ± 69.79 pg/mL for the CXCL12 (–) NHP and 666.13 ± 165.14 pg/mL for the CXCL12 (+) NHP. There was a statistically significant effect noticed in CXCL12 level between 2 NHPs for days 9 and 14 (Figure 3D). We also measured CXCL12 from the peritoneal lavage, normalizing results with dilution factors. At 1 month, the CXCL12 (+) lavage sample showed about a 3-fold higher level of CXCL12 than the CXCL12 (–) lavage sample (Figure 3E). This difference was not evident by the 3-month evaluation, as the levels in the CXCL12 (–) NHP increased significantly by that point. At the 6-month point, the concentration of CXCL12 from the lavage of the CXCL12 (+) animal was about half of the concentration in CXCL12 (–) animal at day 98.

Changes in Populations of PBMCs

A review of changes in population of PBMCs is shown in Results S8 and Figure S4 (**SDC,** http://links.lww.com/TXD/A205).

Postimplantation Effects of Autologous Islet Microbead Implants

Overall Animal Health During Study

Both NHPs receiving the microbead implants recovered quickly from surgery (hemipancreatectomy and autologous islet transplantation) and appeared healthy during the entire period of the study (**Results S9, SDC,** http://links.lww.com/TXD/A205).

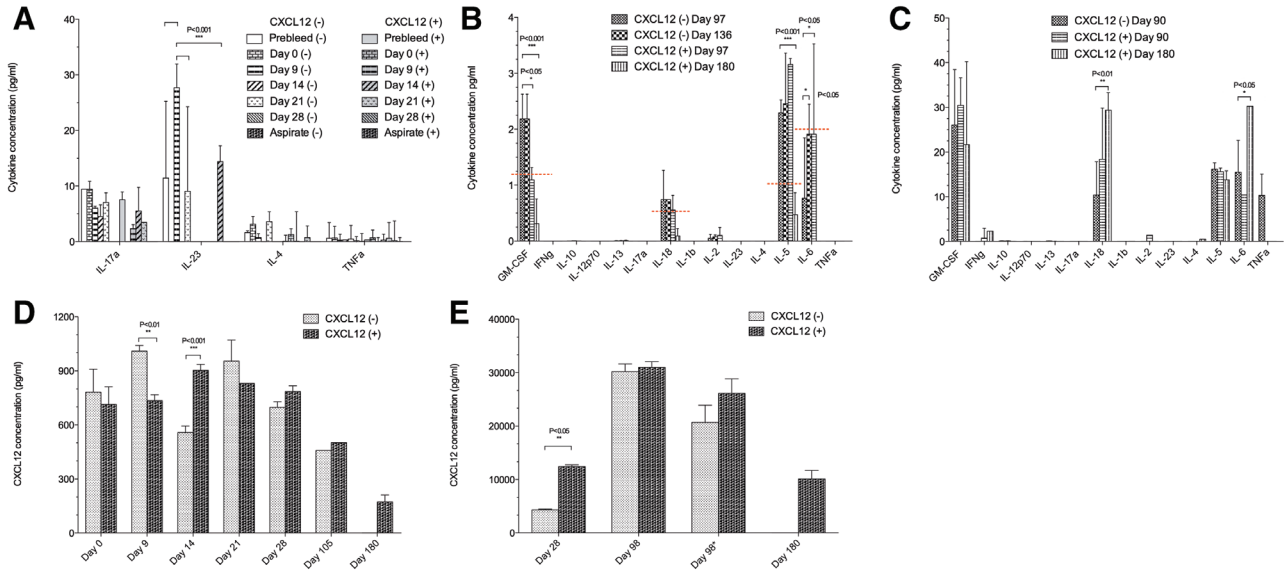

FIGURE 3. Cytokine and CXCL12 concentrations from the CXCL12 (–) and CXCL12 (+) empty microbeads study. Cytokine concentrations from the samples of NHP plasma are shown in A and B, while aspirate samples are shown in C. A, Measurable levels of 4 cytokines (IL-17a, IL-23, IL-4, and tumor necrosis factor-α) in both NHPs at days 0–28, and it appeared that NHP with CXCL12 (–) had a higher level of activation state for these cytokines when compared with the baseline levels. Two-way ANOVA analysis demonstrated for IL-23 significant *P* values (***$P < 0.001$) for prebleed vs day 9, day 9 vs day 21, and day 9 vs day 14. B and C, For days 90, 97, 136, and 180, inflammatory cytokine changes were observed for both CXCL12 (–) and CXCL12 (+) microbeads, both in plasma and intraperitoneal (IP) aspirate. Standard curves for each cytokine were used to extrapolate the concentrations from the FI-background data. Significant *P* values were observed for GM-CSF (***$P < 0.001$, *$P < 0.05$), IL-18 (**$P < 0.01$), IL-5 (***$P < 0.001$), and IL-6 (*$P < 0.05$). The CXCL12 concentrations are shown in D and E. D, The comparison between the CXCL12 (–) and CXCL12 (+) plasma concentrations from days 0 to 180 postimplant. **$P < 0.01$ for day 9, and ***$P < 0.001$ for day 14. E, The aspirate concentrations of CXCL12. The results of 28 days were showing a 3-fold increase in chemokine in the CXCL12 (+) animal, with a **P value < 0.05. The 98-day aspirate samples (*) being stored at –80°C, were assayed twice, and the results demonstrated a decrease in the concentration over time. GM-CSF, granulocyte-macrophage colony-stimulating factor; IL, interleukin; NHP, nonhuman primate.

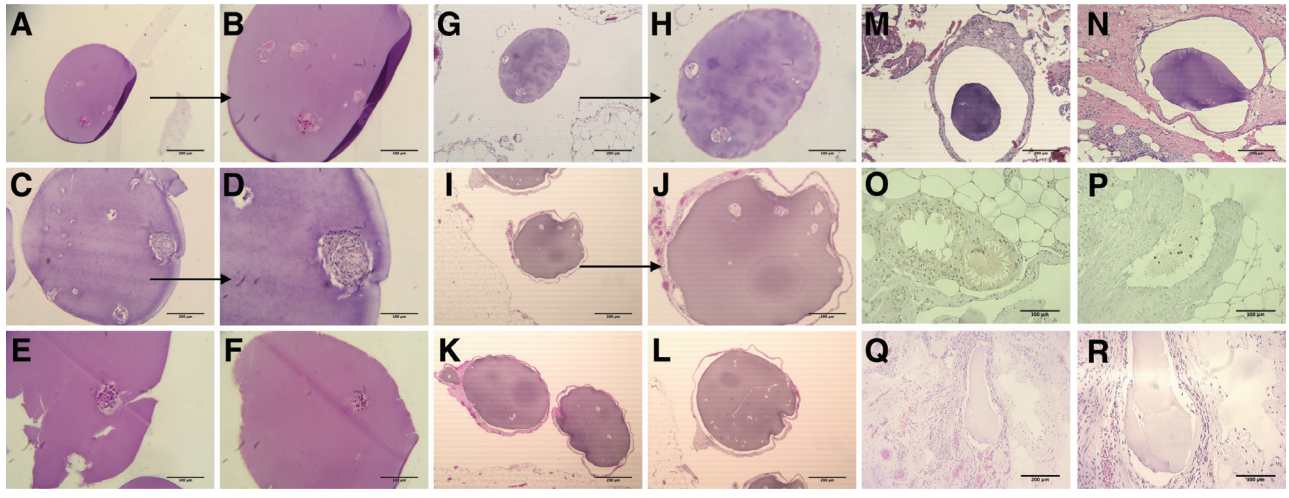

FIGURE 4. Histopathology on explanted free and embedded microbeads from autologous implants at days 30 and 180. A–F, H&E staining of the recovered free microbeads from the first autograft at day 30. Visible nucleated islets and also some denucleated clusters. E, Visible damage from the recovery or staining process. G and H, H&E staining of the tissue-embedded microbeads from the first autograft at day 30. Image showed no cellularization around the capsule but some denucleation of the islets. I–L, H&E staining of the recovered embedded microbeads from the first autograft at day 180. Visible presence of more denucleated islet clusters, but still without significant cellularization. M and N, Histology of the embedded microbeads from the second autograft at day 30. Images showing no cellularization around the capsules. O and P, IHC staining of the embedded microbeads from the second autograft at day 30. Tissues around microbeads stained with antifibroblast demonstrate the presence of the cells and damage to the microbead structure. Q and R, H&E staining of the recovered embedded microbeads from the second autograft at day 180. There were no detectable islet clusters in these microbead samples. H&E, hematoxylin and eosin; IHC, immunohistochemistry.

Changes to Free Microbeads Containing Autologous Islets Posttransplantation

In contrast to the large number of microbeads recovered from the 2 NHPs receiving a empty microbead implant, a single peritoneal lavage of 50 mL in the first animal at 1 month resulted in the recovery of only about 200 microbeads. Microscopic examination of these recovered microbeads showed that 1%–2% were damaged by the aspiration of the lavage. Nevertheless, these recovered microbeads were transparent, retained a smooth and regular morphology, showed no sign of cell infiltration or

fibrosis, and appeared to contain intact islets. After recovery, the mean diameter of the microbeads had increased about 28% (1542 ± 217 μm) compared with the preimplant diameter of 1207±164 μm (Figure S3D, **SDC**, http://links.lww.com/TXD/A205). This increase in size might be caused by prolonged storage in the normal saline used for lavage.

Hematoxylin and eosin staining of these recovered free microbeads showed visible nucleated islets (Figure 4A–F). A subsequent assessment at 6 months resulted in the retrieval of only few free microbeads (n = ~500), all of which appeared to be cellularized (data not shown).

Functional Assessment of Retrieved Encapsulated Autologous Islets

We performed 1- and 24-hour insulin release tests on 8 microbeads, which contained a total of 48 islets (~6 islets per microbead). Insulin release at 1 and 24 hours was 0.46 and 1.17 pM, respectively, per islet, which was dramatically reduced from the amounts of insulin released by encapsulated autologous islets before transplant (447.78 and 1689.58 pM, respectively). We note that before these tests the microbeads had been stored for 3 hours at 4°C in the normal saline-containing lavage fluid that was aspirated from the peritoneum along with the microbeads. The prolonged storage of the islets in this fluid may have imposed additional hypoxic stress that affected the levels of insulin release from the encapsulated islets.

In the second animal, at the 1-month assessment only about 100 microbeads were recovered after a 100-mL lavage. These recovered microbeads had increased in diameter by about 30% (870 ± 69 μm) and retained a high degree of roundness (0.964%) (Figure S3J, **SDC**, http://links.lww.com/TXD/A205). These microbeads showed evidence of intact islets, although both the number and size of islets appeared to have decreased significantly (~60%–80%) compared with preimplantation. By day 180, no free microbeads could be retrieved from the recipient.

Changes to Peritoneum

At the 1-month postimplant evaluation, the peritoneal cavity of the first autologous islet recipient appeared normal and healthy; islet-containing microbeads were clearly visible on the peritoneal tissues (Figure S3E and F, **SDC**, http://links.lww.com/TXD/A205). Microbeads were found throughout the peritoneal cavity and similar to previously did not accumulate or aggregate together in the Pouch of Douglas. The situation with the second animal was quite different. At the 1-month assessment, the NHP had obvious indications of fat-necrotizing pancreatitis secondary to the hemipancreatectomy procedure; this was more visible at the 6-month biopsy (Figure S3K–S3L, **SDC**, http://links.lww.com/TXD/A205). This complication of surgery negatively affected the condition of the microbeads in the peritoneum, as discussed below.

Changes to Embedded Microbeads

Tissue histology showed similar results to the visual microscopic inspection; there was no evidence of cellularization or fibrosis on any of the microbeads (Figure 4G and H). Islets stained positively in some of the microbeads. Many islets appeared to contain an extensive number of denucleated cells. In the first autologous islet microbead recipient, tissue biopsies at 6 months showed the presence of cellularized and likely fibrosed microbeads with few islets that, when present, were mostly necrotic (Figure 4I–L).

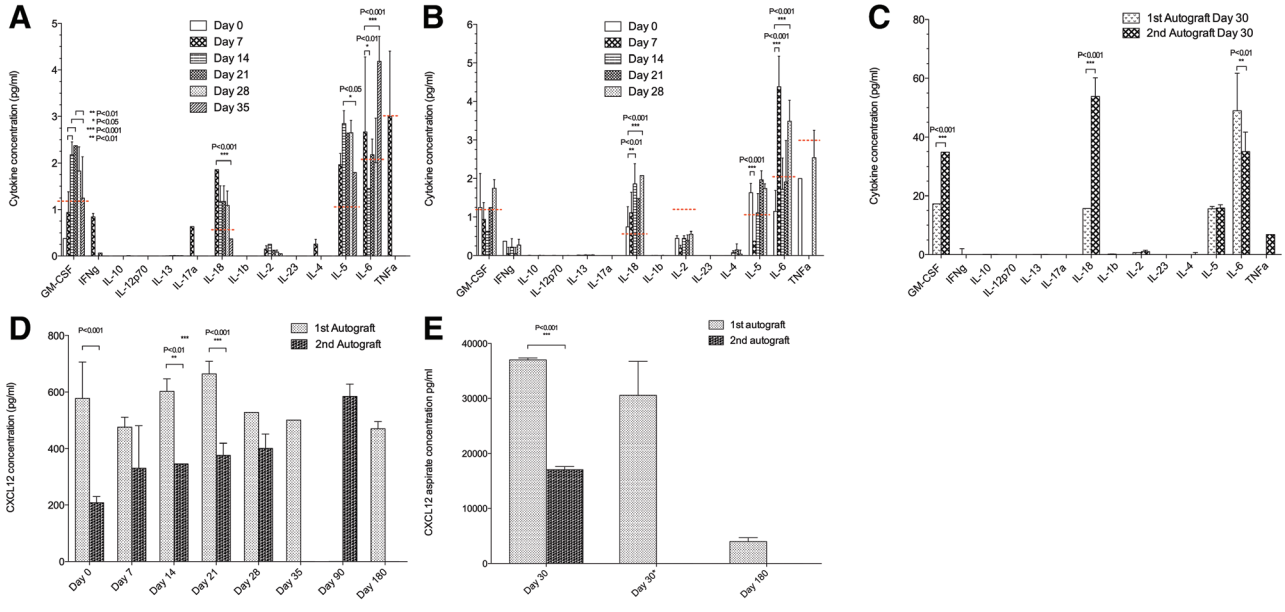

FIGURE 5. Cytokine and CXCL12 concentrations from the autograft microbeads study. A–C, Plasma and aspirate cytokine concentrations from the first and second NHP autografts, days 0–30. The levels of GM-CSF, IL-18, IL-5, and IL-6 increased about 1.5–2× for both autografts when compared with the baseline levels. Two-way ANOVA analysis demonstrated various significant *P* values for GM-CSF, IL-18, IL5, and IL-6 when comparing plasma from different time points (A and B) and aspirate for 2 NHPs (C). D and E, Plasma and aspirate concentrations of the CXCL12 in NHPs, days 0–180. D, There was a statistically significant change in the plasma CXCL12 concentrations between 2 animals for days 0, 14, and 21. E, The NHP aspirate concentrations of CXCL12 demonstrated significant change for day 30. Day 30 aspirate sample from the first NHP was assayed twice (*), and the result did not demonstrate a significant decrease in the concentration over time as compared with the blank microbeads samples. There was a much lower concentration of CXCL12 at the 180-day time point. GM-CSF, granulocyte-macrophage colony-stimulating factor; IL, interleukin; NHP, nonhuman primate.

A number of biopsies were also taken from the second NHP at the 1-month evaluation. Histology of the biopsied tissues demonstrated clinical evidence of fat necrosis with accompanying IP inflammation related to the pancreatitis (Figure 4M and N). Tissues stained with anti-fibroblast antibodies (Figure 4O and P) confirmed the presence of the inflammatory process. Due to the fact that all embedded microbeads were cellularized and fibrosed, we did not perform additional biopsies on the second NHP at the 3-month evaluations. Tissues at the 6-month evaluation where embedded beads were found showed extensive cellularization with fibrosis, (Figure 4Q and R).

Changes in Plasma and Peritoneal Cytokine and Chemokine Levels

In comparison to the plasma samples from the NHPs receiving empty microbeads, here up to 9 cytokines showed detectable levels over the course of the study. GM-CSF, IL-18, IL-5, and IL-6 showed significant variation in concentration between different time points for both animals (Figure 5A and B). IL-5 and IL-6 increases seen here were thought to be secondary to the effect of pancreatitis in the second autograft animal. IL-5 in Th2 cells is also coexpressed with GM-CSF, which was also elevated in our study. IL-6 acts as a proinflammatory cytokine and can be secreted by macrophages in response to specific microbial molecules referred to as pathogen-associated molecular patterns. There is a possibility that alginate microbeads being a foreign biological source material to the innate immune system could trigger this cytokine increase. Similar observation was noticed for the aspirate samples with significant variation between animals, shown in Figure 5C. The CXCL12 plasma level demonstrated significant change between 2 animals for days 0, 14, and 21, while the aspirate CXCL12 level change was significant at day 30 (**Results S10, SDC,** http://links.lww.com/TXD/A205; Figure 5D and E). Samples of aspirate were not collected for the second autograft for day 180.

Changes in Populations of PBMCs

A review of changes in population of PBMCs is shown in Results S11 and Figures S5 and 6 (**SDC,** http://links.lww.com/TXD/A205).

DISCUSSION

This study set out to explore in a stepwise manner whether data generated in mice regarding the immune isolating functions of CXCL12 in the context of islet microencapsulation could be reproduced in a small number of NHPs—commencing with the initial study of IP implantation of alginate microbeads with and without CXCL12 and subsequently the IP transplantation of alginate microbeads containing autologous islets with CXCL12. This includes the caveat that alginate beads were made with ultrapure alginate that was shown to have very low levels of endotoxin and very low levels of other immune contaminants.

Alginate is known to contain several key immunocontaminants that can provoke innate immune responses, including lipopolysaccharides, peptidoglycans, lipoteichoic acid, and flagellin.[29,32] We demonstrated that while the alginate used in this study was relatively low in lipopolysaccharides, lipoteichoic acid, and flagellin, the levels of peptidoglycan were about 5 times what would be considered an acceptable limit. The alginate showed the ability to activate both THP-1 cells and HEK-Blue cell lines overexpressing TLR-2 in an immunostimulation assay. Evaluation of the other component of the microbeads, recombinant human CXCL12, showed a purity level of above 92% and an endotoxin level below 1 EU/mg protein. We demonstrated that the additional raw and intermediate materials used in the manufacture of the alginate microbeads also had endotoxin levels below 1 EU/mg or 1 EU/mL. The final test product was therefore highly pure but still had the potential to elicit an immune response against the alginate, making it useful for evaluating the impact of CXCL12 over a prolonged period. Many studies have shown the importance of minimizing immune contaminants from alginate to reduce the induction of innate immune responses against implanted microbeads or microcapsules.[32,33]

In the context of empty microbeads, and in an "n-of-1" -type study, we demonstrated that CXCL12 could mitigate against the adhesion and elements of the foreign body reaction to microbeads locally with regard to the cellularization of beads that reiterated what had been seen in mice.[34] In addition, there was an unexpected impact of CXCL12 on post-implantation intra-abdominal adhesion formation and overall peritoneal reaction to the implant in comparison to empty alginate microbeads without CXCL12.

Over a 6-month period, free microbeads with CXCL12 remained in pristine condition compared with the deterioration that progressively occurred in the CXCL12 (–) microbeads. This phenomenon is interesting in part because it is not likely that the original CXCL12 is retained within the microbead for this amount of time. In a previous study, we estimated that supraclinical levels of CXCL12 remain in the microbeads for a matter of weeks.[5] In a different study, Duncanson and Sambanis[35] suggest that the retention time of significant concentrations of CXCL12 is a matter of days. In any case, a shorter-term release of CXCL12 from alginate microbeads appears to result in long-term control of the local and systemic inflammatory response to microbeads in the IP cavity. The phenomenon we saw with these empty beads, even those without CXCL12, was significantly different than the rapid overgrowth and tissue embedding described by others for microsphere implantations in NHPs.[36,37] These teams indicated that alginate microbeads at approximately the size we used, when introduced intraperitoneally into NHPs, were embedded into the omental tissue and fat by 7–14 days. In our case, most implanted microbeads were still free of cellular overgrowth at 1 month. There are few other published comparators for this effect, as most investigators have used multishell microcapsules with polylysine or polyornithine, which, if optimized, are not very adherent.[38-40]

This unexpected long-term effect of CXCL12 appears to go beyond the preservation of the microbeads themselves, as the CXCL12 (+) microbeads appeared to reduce the number of adhesions in the peritoneum and the development of fibrosis in the tissues. Again, few differences were noted between the 2 animals at the 1-month assessment point. However, at 3 and 6 months, the peritoneum of the NHP receiving CXCL12 (–) microbeads showed increasing evidence of patchy fibrosis and development of adhesions. These were absent in the peritoneum of the NHP receiving the CXCL12 (+) microbeads. It is possible that these differences were related to an increase in the peritoneal concentration of CXCL12 in the NHP receiving the

CXCL12 (+) microbeads, or due to the increase in foreign body responses in the NHP receiving the CXCL12 (–) microbeads, or a combination of both. While no statistically significant circulating levels of CXCL12 were seen in either animal, there appeared to be about a 3 times greater level of CXCL12 in the lavage fluid of the CXCL12 (+) microbead recipient at 1 month than the CXCL12 (–) microbead recipient. It is hard to draw firm conclusions from this 1 set of samples, especially because there are no baseline levels of CXCL12 in the peritoneum to use as a comparison. However, the time at which this peak level occurred in the peritoneal lavage certainly matched the time period of significant release for the CXCL12 from the alginate microbeads.

While the empty microbead implantation study shows the potential for encapsulated CXCL12 to enhance the isolation of microbeads from the inflammatory and innate immune response, the study of alginate microencapsulated autologous islets in NHPs raised different issues. In the first instance, it is clear that the microencapsulated autologous islet transplantation model is technical, complex, and challenging. First, the partial pancreatectomy has a complication rate in NHPs, including the development of acute pancreatitis associated with the residual pancreas, which was revealed clinically by evidence of IP inflammation, peripancreatic fat necrosis, and slight elevations in pancreatic markers in the second NHP. Second, partial pancreatectomy, islet isolation, microencapsulation, and implantation are mandated to be completed on the same day in the same NHP. This means that the quality control on islet preparations, microencapsulation, and implantation must consequently occur with the NHP maintained under a prolonged (6–8 hours) period of anesthesia while all relevant procedures are completed. Finally, and most significantly, the microencapsulated autologous islet implantation procedure involves the placement of the microbeads into an inflamed and postsurgical site—namely, the IP cavity of an NHP postpartial pancreatectomy. This sets a confoundingly high bar for the CXCL12 effect on the inflammatory and immune isolation of the microbead graft to reach. We suggest that the second NHP demonstrated all of these negative impacts on microbead transplantation because of the evident postpartial pancreatectomy pancreatitis. Interestingly, there was clear evidence that microbeads remained transilluminable without cellular encasement up to 3 months in the first NHP, but it was clear that the autologous islets themselves showed greatly reduced function at both 3 and 6 months postimplantation. Therefore, while in concept autologous islet transplantation in the NHP would remove the variable of anti-islet immune responses from the model, in execution it is likely far more invasive and induces a significant postsurgical inflammatory response and adds a potentially significant confounding factor in the studies.

This study may also demonstrate the limits to the ability of CXCL12 to aid adult autologous islets surviving nonimmune environmental changes. After implantation, islets are vulnerable to stresses such as hypoxia,[41-45] local cytokine release,[46,47] and the effects of hyperglycemia.[48,49] These can cause loss of islet function and death, even without an innate or adaptive immune attack. Here, both sets of autologous islet implants appear to have been affected by postimplant stressors. In the absence of indications of cellularization, fibrosis, or innate immune response to the free microbeads, the encapsulated islets showed a significant decrease in the number of visible islets, islet size, and insulin release. Histology indicated that most intact islet clusters were partially or largely anucleated. In the first autologous graft recipient, this outcome might have been in part due to the suboptimal encapsulation that resulted in 4–5 islets per bead and a larger bead size, both of which can result in hypoxic states.[41,50,51] While a recent study has suggested that microbead size may not have a negative impact on islet survival,[37] a number of other studies suggest that microbeads are most effective when the maximum distance between the islet and the bead surface is <150 μm and that larger microbeads present challenges to islet viability.[44,52-56] As a result, multiple islets within a larger microbead would have been competing for nutrients and oxygen where the microbeads did not have direct vascular access and where oxygen tensions are relatively low.[44,57]

One significant unanswered issue from this study is related to the long-term fate of the majority of implanted alginate microbeads. Historically, there have been concerns about the stability of alginate microbeads crosslinked with calcium ions. Some studies suggest that when calcium alone is used as a crosslinking ion, it can be replaced over time by sodium ions, resulting in the dissolution of the microbeads.[58] Consequently, some investigators have utilized barium or strontium alone or in combination with calcium as crosslinking ions.[59] Evidence from this study on the long-term stability of these calcium-crosslinked microbeads is ambiguous. First, while the alginate microbeads appeared to swell after placement in the peritoneum by 28%–44%, reflecting the presence of sodium ions in the peritoneal fluid and in the lavage solution, this size change remained constant over a period of months and therefore may not signal instability for the microbeads. In both animals, some free microbeads were recoverable up through the 6-month period. At this assessment, the CXCL12 (–) microbeads showed more variation in size and shape that could suggest instability of the beads. However, there were very little indications of instability in the CXCL12 (+) sample, where free microbeads appeared as pristine as the day they were implanted. It may be that the use of CXCL12 in the alginate promotes stability of the bead. CXCL12 can ionically bind to guluronate units within alginate,[60] and this ionic binding may serve to enhance the long-term stability of calcium-crosslinked alginate microbeads.

Together, the data from this n-of-1-type study examining the function of empty and autologous islet microbead studies in NHPs support the next step in our project, which includes alloislet and xenoislet transplantation into nondiabetic NHPs. These results provide support for the utility of CXCL12 in immunomodulation for these types of alginate microbeads, highlight the continued importance of the high purity of alginate and other microbead components, and help to identify key parameters to address any hurdles to overcome in future studies. These most notably include the need for optimization and standardization of the islet and islet microbead preparation process and the challenges of sustaining islet functional survival in the face of nonimmune stressors including the inflammatory response to the microbeads and hypoxia.

In addition, the study demonstrates that studies of this type involving very small numbers of NHPs can reveal important technical and scientific issues that need to be addressed in subsequent appropriately statistically powered studies as this approach to islet transplantation is developed toward first in human studies.

REFERENCES

1. Saravanan PB, Loganathan G, Bashoo N, et al. Clinical islet cell transplantation—recent advances. *Current Science*. 2017;113:1267–1276.

2. Dufrane D, Goebbels RM, Saliez A, et al. Six-month survival of microencapsulated pig islets and alginate biocompatibility in primates: proof of concept. *Transplantation.* 2006;81:1345–1353.
3. Dufrane D, Goebbels RM, Gianello P. Alginate macroencapsulation of pig islets allows correction of streptozotocin-induced diabetes in primates up to 6 months without immunosuppression. *Transplantation.* 2010;90:1054–1062.
4. Elliott RB, Escobar L, Tan PL, et al. Intraperitoneal alginate-encapsulated neonatal porcine islets in a placebo-controlled study with 16 diabetic cynomolgus primates. *Transplant Proc.* 2005;37:3505–3508.
5. Chen T, Yuan J, Duncanson S, et al. Alginate encapsulant incorporating CXCL12 supports long-term allo- and xenoislet transplantation without systemic immune suppression. *Am J Transplant.* 2015;15:618–627.
6. Lim F, Sun AM. Microencapsulated islets as bioartificial endocrine pancreas. *Science.* 1980;210:908–910.
7. Buder B, Alexander M, Krishnan R, et al. Encapsulated islet transplantation: strategies and clinical trials. *Immune Netw.* 2013;13:235–239.
8. Bidarra SJ, Barrias CC, Granja PL. Injectable alginate hydrogels for cell delivery in tissue engineering. *Acta Biomater.* 2014;10:1646–1662.
9. Anker SD, Coats AJ, Cristian G, et al. A prospective comparison of alginate-hydrogel with standard medical therapy to determine impact on functional capacity and clinical outcomes in patients with advanced heart failure (AUGMENT-HF trial). *Eur Heart J.* 2015;36:2297–2309.
10. Szekalska M, Puciłowska A, Szymańska E, et al. Alginate: Current Use and Future Perspectives in Pharmaceutical and Biomedical Applications. *Int J Polymer Sci*. 2016:7697031.
11. Mallett AG, Korbutt GS. Alginate modification improves long-term survival and function of transplanted encapsulated islets. *Tissue Eng Part A.* 2009;15:1301–1309.
12. Orive G, Ponce S, Hernández RM, et al. Biocompatibility of microcapsules for cell immobilization elaborated with different type of alginates. *Biomaterials.* 2002;23:3825–3831.
13. de Vos P, Hoogmoed CG, Busscher HJ. Chemistry and biocompatibility of alginate-PLL capsules for immunoprotection of mammalian cells. *J Biomed Mater Res.* 2002;60:252–259.
14. De Vos P, De Haan BJ, Wolters GH, et al. Improved biocompatibility but limited graft survival after purification of alginate for microencapsulation of pancreatic islets. *Diabetologia.* 1997;40:262–270.
15. Ghulam M. Alginate microparticles for biodelivery: a review. *Afr JPharm Pharmacol*. 2011;5:2726–2737.
16. Mazzitelli S, Tosi A, Balestra C, et al. Production and characterization of alginate microcapsules produced by a vibrational encapsulation device. *J Biomater Appl.* 2008;23:123–145.
17. Mazumder MA, Burke NA, Shen F, et al. Core-cross-linked alginate microcapsules for cell encapsulation. *Biomacromolecules.* 2009;10:1365–1373.
18. Papeta N, Chen T, Vianello F, et al. Long-term survival of transplanted allogeneic cells engineered to express a T cell chemorepellent. *Transplantation.* 2007;83:174–183.
19. Righi E, Kashiwagi S, Yuan J, et al. CXCL12/CXCR4 blockade induces multimodal antitumor effects that prolong survival in an immunocompetent mouse model of ovarian cancer. *Cancer Res.* 2011;71:5522–5534.
20. McCandless EE, Wang Q, Woerner BM, et al. CXCL12 limits inflammation by localizing mononuclear infiltrates to the perivascular space during experimental autoimmune encephalomyelitis. *J Immunol.* 2006;177:8053–8064.
21. Cowley MJ, Weinberg A, Zammit NW, et al. Human islets express a marked proinflammatory molecular signature prior to transplantation. *Cell Transplant.* 2012;21:2063–2078.
22. Jin DK, Shido K, Kopp HG, et al. Cytokine-mediated deployment of SDF-1 induces revascularization through recruitment of CXCR4+ hemangiocytes. *Nat Med.* 2006;12:557–567.
23. Castilla DM, Liu ZJ, Tian R, et al. A novel autologous cell-based therapy to promote diabetic wound healing. *Ann Surg.* 2012;256:560–572.
24. Xu X, Zhu F, Zhang M, et al. Stromal cell-derived factor-1 enhances wound healing through recruiting bone marrow-derived mesenchymal stem cells to the wound area and promoting neovascularization. *Cells Tissues Organs.* 2013;197:103–113.
25. Liu Z, Habener JF. Stromal cell-derived factor-1 promotes survival of pancreatic beta cells by the stabilisation of beta-catenin and activation of transcription factor 7-like 2 (TCF7L2). *Diabetologia.* 2009;52:1589–1598.
26. Hocking AM. The role of chemokines in mesenchymal stem cell homing to wounds. *Adv Wound Care (New Rochelle).* 2015;4(11):623–630.
27. Hanson SE. Mesenchymal stem cells: a multimodality option for wound healing. *Adv Wound Care (New Rochelle).* 2012;1:153–158.
28. Klinker MW, Wei CH. Mesenchymal stem cells in the treatment of inflammatory and autoimmune diseases in experimental animal models. *World J Stem Cells.* 2015;7:556–567.
29. Paredes-Juarez GA, de Haan BJ, Faas MM, et al. A technology platform to test the efficacy of purification of alginate. *Materials (Basel).* 2014;7:2087–2103.
30. Micheal Whelehan. Buchi Encapsulator B-390/B-395, Flawil, Switzerland: BÜCHI Labortechnik AG, 2014.
31. Buchi Operation Manual Encapsulator B-395 Pro, Flawil, Switzerland: BÜCHI Labortechnik AG, 2016.
32. Paredes Juárez GA, Spasojevic M, Faas MM, et al. Immunological and technical considerations in application of alginate-based microencapsulation systems. *Front Bioeng Biotechnol.* 2014;2:26.
33. Ménard M, Dusseault J, Langlois G, et al. Role of protein contaminants in the immunogenicity of alginates. *J Biomed Mater Res B Appl Biomater.* 2010;93:333–340.
34. Hanahan D, Lanzavecchia A, Mihich E. Fourteenth annual pezcoller symposium: the novel dichotomy of immune interactions with tumors. *Cancer Res.* 2003;63:3005–3008.
35. Duncanson S, Sambanis A. Dual factor delivery of CXCL12 and exendin-4 for improved survival and function of encapsulated beta cells under hypoxic conditions. *Biotechnol Bioeng.* 2013;110:2292–2300.
36. Vaithilingam V, Kollarikova G, Qi M, et al. Effect of prolonged gelling time on the intrinsic properties of barium alginate microcapsules and its biocompatibility. *J Microencapsul.* 2011;28:499–507.
37. Veiseh O, Doloff JC, Ma M, et al. Size- and shape-dependent foreign body immune response to materials implanted in rodents and nonhuman primates. *Nat Mater.* 2015;14:643–651.
38. Safley SA, Cui H, Cauffiel S, et al. Biocompatibility and immune acceptance of adult porcine islets transplanted intraperitoneally in diabetic NOD mice in calcium alginate poly-L-lysine microcapsules versus barium alginate microcapsules without poly-L-lysine. *J Diabetes Sci Technol.* 2008;2:760–767.
39. Dagbert F, McConnell YJ, Carmona E, et al. Intraperitoneal distribution of alginate microcapsules in mice. *Modern Chemotherapy*. 2014;3:1–4.
40. Spasojevic M, Paredes-Juarez GA, Vorenkamp J, et al. Reduction of the inflammatory responses against alginate-poly-L-lysine microcapsules by anti-biofouling surfaces of PEG-b-PLL diblock copolymers. *PLoS One.* 2014;9:e109837.
41. Barkai U, Rotem A, de Vos P. Survival of encapsulated islets: more than a membrane story. *World J Transplant.* 2016;6:69–90.
42. Luo LG, Luo JZ. Anti-apoptotic effects of bone marrow on human islets: a preliminary report. *J Stem Cell Res Ther*. 2015;5. pii:274.
43. Kanak MA, Takita M, Kunnathodi F, et al. Inflammatory response in islet transplantation. *Int J Endocrinol.* 2014;2014:451035.
44. Suszynski TM, Avgoustiniatos ES, Papas KK. Oxygenation of the intraportally transplanted pancreatic islet. *J Diabetes Res.* 2016;2016:7625947.
45. Pedraza E, Coronel MM, Fraker CA, et al. Preventing hypoxia-induced cell death in beta cells and islets via hydrolytically activated, oxygen-generating biomaterials. *Proc Natl Acad Sci U S A.* 2012;109:4245–4250.
46. Abdulreda MH, Berggren PO. Islet inflammation in plain sight. *Diabetes Obes Metab.* 2013;15(Suppl 3):105–116.
47. Russell MA, Morgan NG. The impact of anti-inflammatory cytokines on the pancreatic β-cell. *Islets.* 2014;6:e950547.
48. Fonseca SG, Gromada J, Urano F. Endoplasmic reticulum stress and pancreatic β-cell death. *Trends Endocrinol Metab.* 2011;22:266–274.
49. Dai C, Li Y, Yang J, et al. Hepatocyte growth factor preserves beta cell mass and mitigates hyperglycemia in streptozotocin-induced diabetic mice. *J Biol Chem.* 2003;278:27080–27087.
50. Williams SJ, Huang HH, Kover K, et al. Reduction of diffusion barriers in isolated rat islets improves survival, but not insulin secretion or transplantation outcome. *Organogenesis.* 2010;6:115–124.
51. Buchwald P. A local glucose-and oxygen concentration-based insulin secretion model for pancreatic islets. *Theor Biol Med Model*. 2011;8:20.
52. Lehmann R, Zuellig RA, Kugelmeier P, et al. Superiority of small islets in human islet transplantation. *Diabetes.* 2007;56:594–603.
53. Ichihara Y, Utoh R, Yamada M, et al. Size effect of engineered islets prepared using microfabricated wells on islet cell function and arrangement. *Heliyon.* 2016;2:e00129.

54. Fotino N, Fotino C, Pileggi A. Re-engineering islet cell transplantation. *Pharmacol Res.* 2015;98:76–85.
55. Hilderink J, Spijker S, Carlotti F, et al. Controlled aggregation of primary human pancreatic islet cells leads to glucose-responsive pseudoislets comparable to native islets. *J Cell Mol Med.* 2015;19:1836–1846.
56. Tomei AA, Manzoli V, Fraker CA, et al. Device design and materials optimization of conformal coating for islets of langerhans. *Proc Natl Acad Sci U S A.* 2014;111:10514–10519.
57. Buchwald P. FEM-based oxygen consumption and cell viability models for avascular pancreatic islets. *Theor Biol Med Model.* 2009;6:5.
58. Forster RE, Thürmer F, Wallrapp C, et al. Characterisation of physico-mechanical properties and degradation potential of calcium alginate beads for use in embolisation. *J Mater Sci Mater Med.* 2010;21:2243–2251.
59. Cappai A, Petruzzo P, Ruiu G, et al. Evaluation of new small barium alginate microcapsules. *Int J Artif Organs.* 1995;18:96–102.
60. Wang Y, Irvine DJ. Engineering chemoattractant gradients using chemokine-releasing polysaccharide microspheres. *Biomaterials.* 2011;32:4903–4913.